Available online at www.sciencedirect.com

ScienceDirect

Procedia Structural Integrity 33 (2021) 207–214

Structural Integrity Procedia

www.elsevier.com/locate/procedia

IGF26 – 26th International Conference on Fracture and Structural Integrity

Fracture parameters of alkali-activated aluminosilicate composites with ceramic precursor: durability aspects

Hana Šimonová[a,*], Martin Lipowczan[a], Iva Rozsypalová[a], Petr Daněk[a], David Lehký[a], Pavla Rovnaníková[a], Zbyněk Keršner[a]

[a]*Brno University of Technology, Faculty of Civil Engineering, Veveri 331/95, Brno 602 00, Czech Republic*

Abstract

Four sets of alkali-activated aluminosilicate (AAAS) composites based on ceramic precursors were studied in terms of their characterization by mechanical fracture parameters as a basis for considerations of durability. AAAS composites made of brick powder as a precursor and alkaline activator with various silicate moduli (M_s = 0.8, 1.0, 1.2, 1.4, and 1.6) were investigated. The sets of AAAS composites differed in terms of the used filler: quartz sand or brick rubble. Two different precursor particle size ranges of 0–1 mm and 0–0.3 mm were used for both types of filler. The test specimens had nominal dimensions of 40 × 40 × 160 mm and were provided with a notch at midspan after 28 days of hardening. The notches were cut up to 1/3 of the height of the specimens. The specimens were subjected to three-point bending fracture tests during which force vs. deflection (*F–d*) and force vs. crack mouth opening displacement (*F–CMOD*) diagrams were recorded. Tensile strength $f_{t,ID}$ and specific fracture energy $G_{F,ID}$ values were identified using the inverse method based on a neural network ensemble. The obtained *F–CMOD* diagrams were subsequently evaluated using the double-*K* fracture model supported by the $f_{t,ID}$ and $G_{F,ID}$ values. The double-*K* model allows the quantification of two different levels of crack propagation: initiation, which corresponds to the beginning of stable crack growth, and unstable crack propagation.

Keywords: Alkali-activated aluminosilicate; artificial neural network; neural network ensemble; crack initiation; double-*K* model; fracture test; force–displacement diagram; mechanical fracture parameters.

* Corresponding author. Tel.: +420 541 147 381.
E-mail address: simonova.h@vutbr.cz

10.1016/j.prostr.2021.10.025

1. Introduction

Alkali-activated aluminosilicate (AAAS) composites are specific materials characterized by the absence of cement, a substance which has a significant impact on the environment. These composites consist of an aluminosilicate material as a precursor, an alkaline activator, a sodium or potassium silicate solution adjusted to a suitable silicate modulus, and a filler such as quartz sand or inert waste materials. The properties of AAAS composites based on brick dust and potassium silicate as an activator are described in many papers (Bayer and Rovnaníková, 2018; Kumpová et al., 2019; Šimonová et al., 2020, etc.).

Wang et al. (2020) see the advantages of AAAS materials compared to those based on Portland cement as lying in their energy-saving and environmentally friendly properties. They compared AAAS materials containing different calcium contents in the precursor to concrete based on Portland cement, subjecting them to sulfate attack, acid corrosion, carbonation, and chloride penetration. Although both types of material were damaged by the corrosive environments they were exposed to, in general, AAAS materials were found to have higher durability than Portland cement-based materials.

The investigation of durability by monitoring the effect of corrosion factors on AAAS materials is time-consuming. In our research, an attempt was made to choose other aspects of durability evaluation based on the analysis of mechanical fracture parameters, especially those parameters that describe the resistance of the material to failure initiation.

2. Experimental part

2.1. Materials and specimens

Waste brick powder from the brick grinding process was used as aluminosilicate material for the preparation of AAAS composites. The waste material is produced by a brick kiln located in the Czech Republic (HELUZ cihlářský průmysl v.o.s., Libochovice). The waste brick material was dried at a temperature of 105 °C to a constant weight and then sieved using a 4 mm sieve. Subsequently, the powder was ground in a ball mill to two grain sizes: less than 1 mm, and less than 0.3 mm. Three fractions were thus obtained: 0–0.3 mm, 0–1 mm, and 1–4 mm. The first and second fractions (brick powder) were used as a precursor; the third fraction (brick rubble) was eventually used as filler. The two different precursor particle size ranges (0–1 mm and 0–0.3 mm) were both used in the experiment. Potassium water glass (produced by Vodní sklo, a. s., Czech Republic) containing 26.23 % SiO_2 and 12.06 % K_2O was used as an alkaline activator. The waste brick powder was mixed with modified solutions of potassium water glass with silicate moduli (SiO_2/K_2O) of M_s = 0.8, 1.0, 1.2, 1.4, and 1.6. The potassium alkaline activator was selected due to the resultant lower tendency of the hardened composite to exhibit efflorescence.

A total of four sets of AAAS composites were studied. Two different fillers were added to the mixtures. Quartz sand composed of three fractions (PG1 0.063–1.00 mm, PG2 0.25–4.00 mm, and PG3 1.00–4.00 mm) in a ratio of 1:1:1 was used in the first and second set of AAAS composites, while brick rubble with a fraction of 1–4 mm was used for the third and fourth set of AAAS composites. For one batch of waste brick powder (1 000 g), 450 g potassium silicate (potassium water glass) was used along with five different amounts of potassium hydroxide (219.5 g, 162.5 g, 125.0 g, 98.0 g, and 78.0 g), and 1 050 g of quartz sand or brick rubble. Water was added in the amount needed to give the mixtures the same consistency. In these mixtures, the S/Al ratio was 4.07. Specimens with nominal dimensions of 40 × 40 × 160 mm were prepared. After hardening, the specimens were removed from their molds, wrapped in PE foil, and stored until the fracture tests were performed.

2.2. Fracture tests

The fracture experiments in the three-point bending configuration (see Fig. 1, left) were conducted when the AAAS composites were at the age of 28 days. The above-mentioned prismatic specimens were provided with an initial central edge notch one day before testing. The notch length was approximately one-third of the specimen's height. The span length was set to 140 mm. The specimen with the stress concentrator was loaded in opening mode – mode I. A LabTest 6.250 stiff multi-purpose mechanical testing machine with a load range of 0−250 kN was used for the fracture tests.

The loading process was controlled by a constant increment of displacement of 0.02 mm/min over the whole course of the experiment.

The vertical force (F), the vertical displacement (d) (measured in the middle of the span length using an inductive sensor), and the crack mouth opening displacement ($CMOD$) (measured using a strain gauge mounted between blades fixed on the bottom surface of the specimen) were recorded during the experiment. This allowed continuous records to be obtained for the fracture tests in the form of $F–d$ and $F−CMOD$ diagrams.

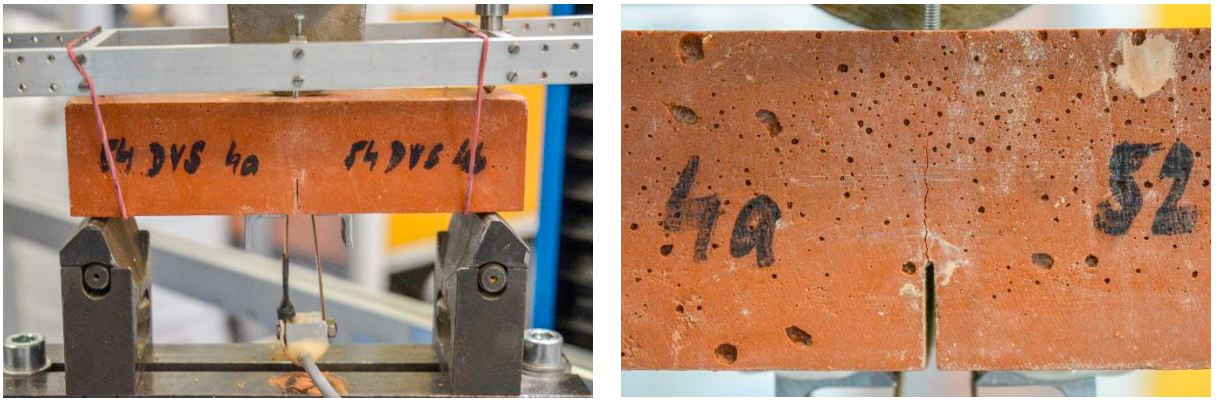

Fig. 1. Illustration of the three-point bending fracture test configuration (left) and detail of a test specimen with a magistral crack (right).

3. Methods

3.1. Identification of selected mechanical fracture parameters

Values were identified for modulus of elasticity E_{ID}, tensile strength $f_{t,ID}$, and specific fracture energy $G_{F,ID}$ via inverse analysis based on a neural network ensemble (NNE). The inverse procedure originally developed by Novák and Lehký (2006) transforms fracture test response data into the desired mechanical fracture parameters. This approach is based on matching laboratory measurements with the results gained by reproducing the same test numerically (Lehký et al., 2014). The ATENA FEM program (Červenka et al., 2016) was employed for the numerical simulation of the fracture test. The 3DNonLinearCementitious2 material model was selected to govern the gradual evolution of localized damage. The cornerstone of the inverse method is an ensemble of artificial neural networks (ANNs), which is used as a surrogate model of an unknown inverse function between the input mechanical fracture parameters and the corresponding response parameters. The individual ANNs are used (activated) separately or in the form of an NNE, depending on the response – the force vs. displacement diagram – of the identified specimen. The best strategy that achieves the most accurate results for a wide range of material parameters while maintaining reasonable computational demands is automatically selected. For a detailed description of the NNE-based inverse analysis method, see Lehký et al. (2019). The obtained $f_{t,ID}$, and $G_{F,ID}$ values will be used as input parameters in the double-K fracture model.

3.2. Double-K fracture model

The double-K fracture (DKF) model (Kumar and Barai, 2011) was chosen for the evaluation of the obtained $F–CMOD$ diagrams. The input values from the recorded $F–CMOD$ diagrams are maximum force F_{max} and matching crack mouth opening displacement $CMOD_{Fmax}$, as well as the vertical force in the ascending linear part of the diagram F_i and the matching crack mouth opening displacement $CMOD_{Fi}$. The DKF model works using a combination of the concept of the cohesive forces on the fictitious crack with a criterion based on the stress intensity factor. The different stages of the fracture process in materials with a brittle matrix can be predicted using this model. Two parameters are used for this purpose, namely initial cracking toughness $K_{I,c}^{ini}$ and unstable fracture toughness $K_{I,c}^{un}$, which are given in terms of stress intensity factor. The unstable fracture toughness $K_{I,c}^{un}$ is defined as the critical stress intensity factor, which corresponds to the effective fracture toughness used in the effective crack model by Karihaloo (1995).

The initial cracking toughness $K_{I,c}^{ini}$ stands for the capability to withstand an external load before the origin of crack propagation. The difference between these two parameters is an equivalent stress intensity factor caused by the cohesive forces acting on the fictitious crack, called cohesive fracture toughness $K_{I,c}^{c}$ (Xu and Reinhardt, 1999). In this paper, the unstable fracture toughness $K_{I,c}^{un}$ and the cohesive fracture toughness $K_{I,c}^{c}$ were assessed first, after which the initial cracking toughness $K_{I,c}^{ini}$ was calculated.

The cohesive softening function which characterizes the relationship between cohesive stress and effective crack opening displacement *COD* needs to be defined for the calculation of the cohesive fracture toughness $K_{I,c}^{c}$. In this paper, the nonlinear softening function introduced by Reinhardt et al. (1986) was chosen. The input parameters, namely tensile strength $f_{t,ID}$, and the fracture energy $G_{F,ID}$ of the softening function, were determined from *F–d* diagrams using the above-mentioned NNE-based inverse analysis method. Then, the critical crack opening displacement COD_c was calculated according to the following formula:

$$COD_c = \frac{5.136 \cdot G_{F,ID}}{f_{t,ID}}. \quad (1)$$

4. Results

The undermentioned results are presented in two steps. First, the tables can be used to find the values of selected identified parameters for all four sets of investigated AAAS composites and the values of the DKF model input parameter calculated using them. Subsequently, the figures summarize selected output parameters of the DKF model, structured according to the particle size range of the precursor – coarse (0–1 mm) and fine (0–0.3 mm). The variable in each set of AAAS composites is the silicate modulus. The evaluation always includes the arithmetic mean, usually determined from six measurements, and the variability of the values of the resulting parameters is quantified in the tables using coefficients of variation (CoV) and in the figures using standard deviations (error bars in the graphs).

The parameter values of the nonlinear softening function for all sets of investigated AAAS composites, namely tensile strength $f_{t,ID}$, fracture energy $G_{F,ID}$, and critical crack opening displacement COD_c, are summarized in Table 1, Table 2, and Table 3, respectively.

The resistance to stable crack propagation is represented by initial cracking toughness $K_{I,c}^{ini}$ in Fig. 2, while the resistance to unstable crack propagation is represented by unstable fracture toughness $K_{I,c}^{un}$, which is presented in Fig. 3.

Table 1. Tensile strength in MPa (CoV in %) obtained by identification.

	Silicate modulus (−)				
Composite	0.8	1.0	1.2	1.4	1.6
Brick rubble; precursor 0−1.0 mm	1.53 (8.7)	2.31 (16.5)	1.99 (8.3)	1.62 (20.1)	1.82 (19.2)
Quartz sand; precursor 0−1.0 mm	1.64 (7.9)	1.99 (24.0)	2.43 (7.2)	1.90 (11.8)	1.72 (7.6)
Brick rubble; precursor 0−0.3 mm	0.65 (12.4)	1.25 (15.4)	0.97 (14.2)	1.15 (16.2)	0.91 (14.0)
Quartz sand; precursor 0−0.3 mm	1.03 (8.0)	1.03 (8.4)	1.09 (16.7)	0.94 (7.0)	0.78 (12.0)

Table 2. Fracture energy in J/m^2 (CoV in %) obtained by identification.

	Silicate modulus (−)				
Composite	0.8	1.0	1.2	1.4	1.6
Brick rubble; precursor 0−1.0 mm	61.7 (30.2)	65.5 (14.0)	66.8 (16.3)	70.5 (15.9)	68.8 (14.4)
Quartz sand; precursor 0−1.0 mm	34.4 (29.8)	45.5 (20.3)	56.2 (19.5)	64.1 (20.9)	58.9 (11.3)
Brick rubble; precursor 0−0.3 mm	52.4 (21.8)	57.7 (11.3)	62.0 (13.0)	54.8 (20.2)	62.6 (25.4)
Quartz sand; precursor 0−0.3 mm	29.8 (23.5)	31.9 (10.0	34.3 (13.6)	37.0 (23.6)	37.6 (24.3)

Table 3. Critical crack opening displacement in mm (CoV in %).

	Silicate modulus (−)				
Composite	0.8	1.0	1.2	1.4	1.6
Brick rubble; precursor 0−1.0 mm	0.209 (31.6)	0.154 (30.6)	0.171 (15.9)	0.232 (28.7)	0.201 (24.8)
Quartz sand; precursor 0−1.0 mm	0.112 (22.5)	0.128 (43.6)	0.114 (6.9)	0.178 (23.0)	0.176 (8.8)
Brick rubble; precursor 0−0.3 mm	0.421 (23.9)	0.243 (23.6)	0.335 (24.1)	0.255 (33.6)	0.364 (34.7)
Quartz sand; precursor 0−0.3 mm	0.150 (25.4)	0.160 (15.1)	0.177 (16.0)	0.205 (29.6)	0.249 (20.4)

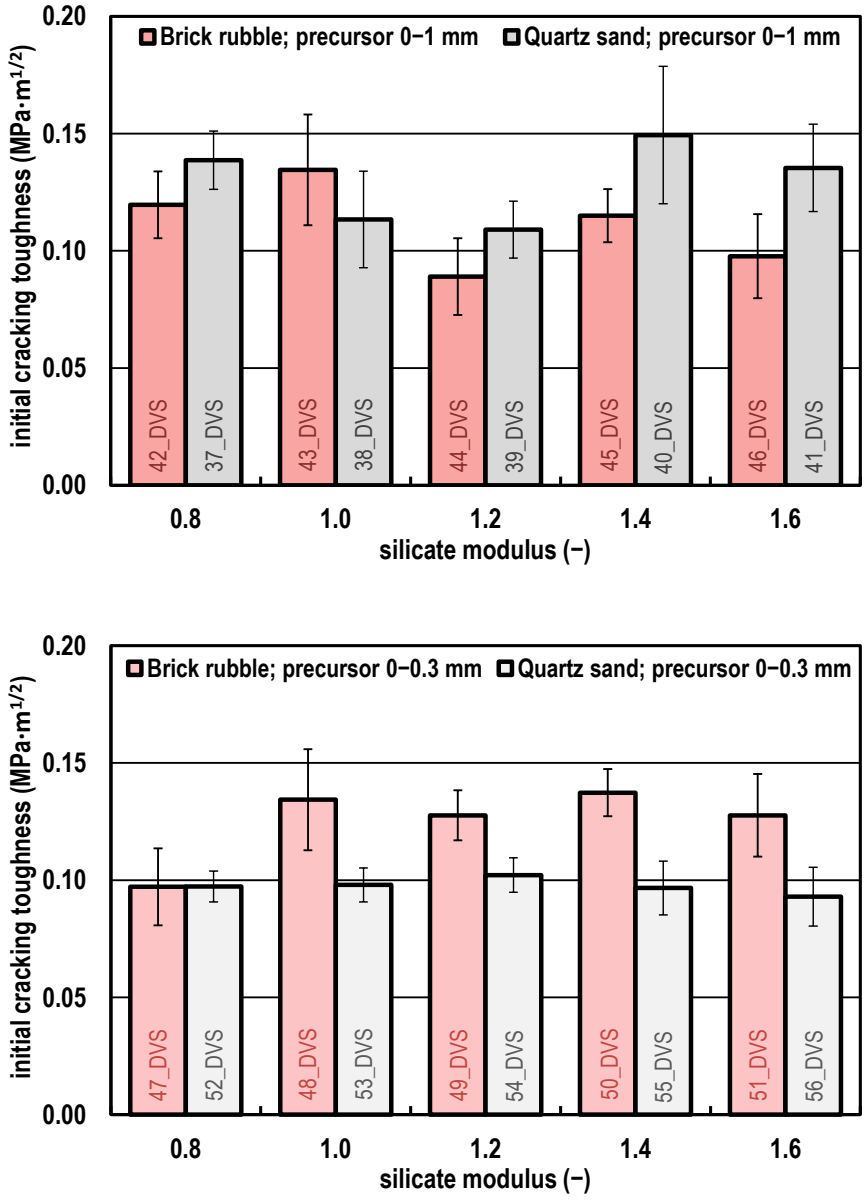

Fig. 2. Initial cracking toughness of investigated sets of AAAS composites.

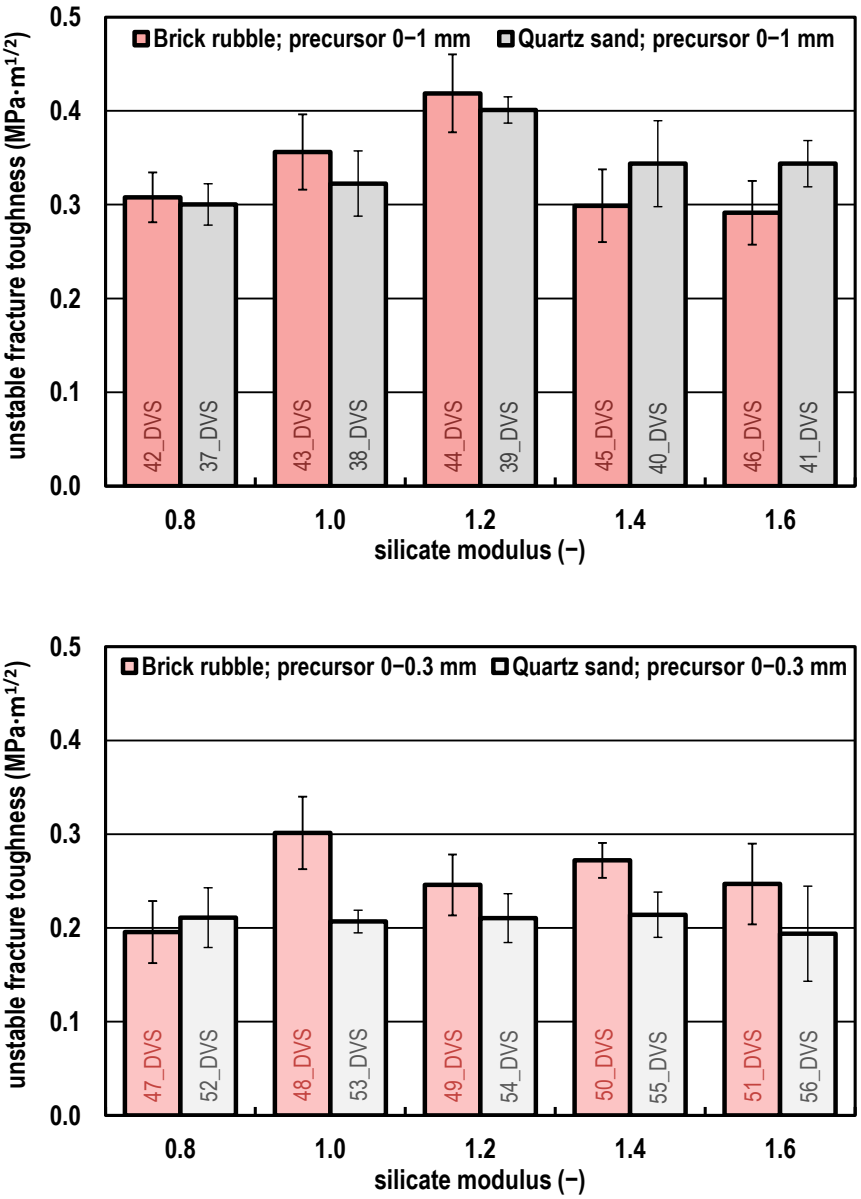

Fig. 3. Unstable fracture toughness of investigated sets of AAAS composites.

Several conclusions can be drawn from the graphs displayed above. The resultant $K_{I,c}^{ini}$ values are more dependent on changes in the silicate modulus and also fluctuate more significantly if the coarse precursor is used. The values (with a few exceptions) are almost the same when the variability of the results is taken into account for the whole range of silicate modulus values and when the fine precursor is used. AAAS composites with quartz sand as filler are generally more resistant to crack initiation in the case of a coarse precursor, while the opposite is true for a fine precursor. In terms of unstable fracture toughness, AAAS composites with the coarse precursor are more significantly resistant. Generally, both monitored parameters show more stable values with changing silicate modulus if the fine precursor is used regardless of the used filler.

The mean values of initial cracking toughness $K_{I,c}^{ini}$ and unstable fracture toughness $K_{I,c}^{un}$ through a whole range of silicate moduli for individual sets of composites are presented in Table 4. The mean values of both investigated parameters increased by about 17 and 4 %, respectively, in the case of composite with coarse precursor if quartz sand was used as aggregate instead of brick rubble, while the precursor with a smaller maximum grain led to reductions in the values of these parameters by about 22 and 18 %, respectively. The highest values were obtained for both parameters for the composite with coarse precursor and quartz sand as a filler. The use of a finer precursor led to reduced values being obtained for the investigated parameters, apart from initial cracking toughness $K_{I,c}^{ini}$ if brick rubble was used as filler.

Table 4. Mean values of initial cracking toughness $K_{I,c}^{ini}$ and unstable fracture toughness $K_{I,c}^{un}$ in MPa·m$^{1/2}$ (CoV in %).

	$K_{I,c}^{ini}$		$K_{I,c}^{un}$	
Composite	Absolute	Relative	Absolute	Relative
Brick rubble; precursor 0−1.0 mm	0.112 (18.7)	100.0 | − | 100.0	0.323 (16.3)	100.0 | − | 100.0
Quartz sand; precursor 0−1.0 mm	0.131 (18.2)	117.0 | − | 100.0	0.337 (12.0)	104.3 | − | 100.0
Brick rubble; precursor 0−0.3 mm	0.125 (16.3)	111.6 | 100.0 | 111.6	0.252 (18.6)	78.0 | 100.0 | 78.0
Quartz sand; precursor 0−0.3 mm	0.097 (9.1)	86.6 | 77.6 | 74.0	0.208 (13.8)	64.4 | 82.5 | 61.7

5. Conclusions

Four sets of AAAS composites with different silicate moduli were studied. They differed in the two precursor size ranges and two fillers used. Thanks to the use of inverse analysis, it was possible to determine values not only for fracture energy but also for tensile strength from the data gained during three-point bending tests. These identified parameters of the tested composites were verified via the direct evaluation of force–displacement diagrams as well as through the comparison of experimental and numerical responses. In all cases, the high accuracy of the values identified by the ensemble of neural networks was confirmed.

The following conclusions can be drawn from the obtained results: (i) The grain size range of the precursor has a significant effect on the values of all identified parameters – tensile strength, fracture energy, and critical crack opening displacement. The use of a precursor with a smaller maximum grain leads to reduced values being obtained for these parameters due to the fact that these composites are more demanding as regards the amount of alkaline solution needed. (ii) In terms of resistance to damage initiation, AAAS composites with coarse precursor and quartz sand filler can be recommended. Based on the obtained results, if brick rubble is used as a filler, a smaller fraction of precursor can be suggested, especially for materials with a higher silicate modulus.

(iii) In terms of unstable fracture toughness, the most durable of the tested materials are AAAS composites with a silicate modulus of 1.2 and with coarse precursor being used as filler in both cases.

The resulting differences in the values of the monitored parameters for the four types of AAAS composites lead to the assumption that stress from, for example, the crystallization pressures of corrosion salts will lead to differences in the durability of these materials. This assumption will be the subject of further investigation.

Acknowledgements

Financial support provided by the Czech Science Foundation (GACR) under project No. 19-01982S (alkali-activated aluminosilicate composites based on ceramic precursors) and No. 19-09491S (MUFRAS, neural network support) is gratefully acknowledged.

References

Bayer, P., Rovnaníková, P., 2018. Effect of alkaline activator quantity and temperature of curing on the properties of alkali-activated brick dust, IOP Conference Series: Materials Science and Engineering 385, 012004.

Červenka, V., Jendele, L., Červenka, J., 2016. ATENA program documentation, Part 1: theory. Cervenka Consulting Ltd., Prague.

Karihaloo, B. L., 1995. Fracture Mechanics and Structural Concrete. Longman Scientific & Technical, New York, pp. 330.

Kumar, S., Barai, S. V., 2011. Concrete Fracture Models and Applications. Springer, Berlin, pp. 262.

Kumpová, I., Rozsypalová, I., Keršner, Z., Rovnaníková, P., Vopálenský, M., 2019. X-ray micro-tomography characterization of voids caused by three-point bending in selected alkali-activated aluminosilicate composite, Acta Polytechnica CTU Proceedings 25, 58−63.

Lehký, D., Keršner, Z., Novák, D., 2014. FraMePID-3PB software for material parameter identification using fracture tests and inverse analysis. Advances in Engineering Software 72, 147–154.

Lehký, D., Lipowczan, M., Šimonová, H., Keršner, Z., 2019. A neural network ensemble for the identification of mechanical fracture parameters of fine-grained brittle matrix composites. The 10th International Conference on Fracture Mechanics of Concrete and Concrete Structures (FraMCoS-X), Bayonne, France.

Novák, D., Lehký, D., 2006. ANN Inverse Analysis Based on Stochastic Small-Sample Training Set Simulation. Engineering Application of Artificial Intelligence 19, 731–740.

Reinhardt, H. W., Cornelissen, H. A. W., Hordijk, D. A., 1986. Tensile tests and failure analysis of concrete. Journal of Structural Engineering 112, 2462–2477.

Šimonová, H., Kumpová, I., Rozsypalová, I., Bayer, P., Frantík, P., Rovnaníková, P., Keršner, Z., 2020. Fracture Parameters of Alkali-activated Aluminosilicate Composites with Ceramic Precursor, Solid State Phenomena: 26th Concrete Days. Trans Tech Publications Ltd, Switzerland, 73–79.

Wang, A., Zheng, Y., Zhang, Z., Liu, K., Li, Y., Shi, L., Sun, D., 2020. The Durability of Alkali-Activated Materials in Comparison with Ordinary Portland Cements and Concretes: A Review. Engineering 6, 695–706.

Xu, S., Reinhardt, H. W., 1999. Determination of double-*K* criterion for crack propagation in quasi-brittle fracture, Part II: Analytical evaluating and practical measuring methods for three-point bending notched beams. International Journal of Fracture 98, 151–177.